J Physiol (2003), **553.2**, *pp.* 545–559
© The Physiological Society 2003
DOI: 10.1113/jphysiol.2003.050419
www.jphysiol.org

Journal of Physiology

Pacing of interstitial cells of Cajal in the murine gastric antrum: neurally mediated and direct stimulation

Elizabeth A. H. Beckett, Cathrine A. McGeough, Kenton M. Sanders and Sean M. Ward

Department of Physiology and Cell Biology, University of Nevada School of Medicine, Reno, NV 89557, USA

Phase advancement of electrical slow waves and regulation of pacemaker frequency was investigated in the circular muscle layer of the gastric antra of wild-type and W/W^V mice. Slow waves in the murine antrum of wild-type animals had an intrinsic frequency of 4.4 cycles min^{-1} and were phase advanced and entrained to a maximum of 6.3 cycles min^{-1} using 0.1 ms pulses of electrical field stimulation (EFS) (three pulses delivered at 3–30 Hz). Pacing of slow waves was blocked by tetrodotoxin (TTX) and atropine, suggesting phase advancement was mediated via intrinsic cholinergic nerves. Phase advancement and entrainment of slow waves via this mechanism was absent in W/W^V mutants which lack intramuscular interstitial cells of Cajal (ICC-IM). These data suggest that neural regulation of slow wave frequency and regulation of smooth muscle responses to slow waves are mediated via nerve–ICC-IM interactions. With longer stimulation parameters (1.0–2.0 ms), EFS phase advanced and entrained slow waves in wild-type and W/W^V animals. Pacing with 1–2 ms pulses was not inhibited by TTX or atropine. These data suggest that stimulation with longer pulse duration is capable of directly activating the pacemaker mechanism in ICC-MY networks. In summary, intrinsic excitatory neurons can phase advance and increase the frequency of antral slow waves. This form of regulation is mediated via ICC-IM. Longer pulse stimulation can directly activate ICC-MY in the absence of ICC-IM.

(Received 3 July 2003; accepted after revision 15 September 2003; first published online 18 September 2003)
Corresponding author S. M. Ward: Department of Physiology and Cell Biology, University of Nevada School of Medicine, Reno, NV 89557, USA. Email: sean@physio.unr.edu

Electrical activity in the gastrointestinal tract is generated by a specialized population of cells known as interstitial cells of Cajal (ICC). In the gastric antrum, slow waves are initiated in ICC in the myenteric region (ICC-MY) and conduct into electrically coupled circular and longitudinal muscle layers (Dickens *et al.* 1999; Ordog *et al.* 1999). A second population of ICC, referred to as intramuscular ICC (ICC-IM), is located within the muscle bundles of circular and longitudinal muscle layers (Burns *et al.* 1996), and these cells are critical for cholinergic and nitrergic neurotransmission in the murine fundus (Burns *et al.* 1996; Ward *et al.* 2000*a*; Beckett *et al.* 2002). Recent studies have also suggested that ICC-IM mediate cholinergic and nitrergic inputs to the circular muscle of the antrum (Hirst *et al.* 2002*c*; Suzuki *et al.* 2003). Analogous morphological associations exist between ICC-IM and enteric motor nerve terminals in the guinea-pig, opossum, cat, dog and human suggesting that ICC-IM may have a common role in neurotransmission in many species (Roman *et al.* 1975; Daniel & Posey-Daniel, 1984; Torihashi *et al.* 1993; Rummesen *et al.* 1993; Wang *et al.* 1999; Horiguchi *et al.* 2002).

There have been suggestions that ICC-MY and ICC-IM have discrete duties, as pacemakers and mediators of neural inputs, respectively (Ward & Sanders, 2001). However, recent studies have begun to question the separation of labour between different populations of ICC. Small bundles of guinea-pig antrum and pylorus can generate rhythmic depolarizations (termed regenerative potentials) in the absence of ICC-MY (Edwards *et al.* 1999; Van Helden *et al.* 2000; Hirst *et al.* 2002*b*), and studies of canine antral muscles have clearly shown that smooth muscle bundles lacking ICC-MY but containing intramuscular and septal ICC (ICC-IM and ICC-SEP) are capable of generating slow wave activity (Horiguchi *et al.* 2001). Hirst and colleagues have also shown that cholinergic nerves innervating guinea-pig antral bundles can initiate events that can induce premature pacemaker potentials in ICC-MY (Hirst *et al.* 2002*c*). Although these authors have previously shown that slow wave activity is normally initiated in ICC-MY (Dickens *et al.* 1999), these findings suggest conduction of impulses from the ICC-IM and/or smooth muscle cells can drive pacemaker events in ICC-MY. Although the exact pathway for the flow of current has not been established, it was presumed that spread of depolarization from ICC-IM through smooth muscle cells to ICC-MY is responsible for evoking premature slow waves.

For many years it has been recognized that electrical pacing can drive the stomach to higher frequencies and

Journal of Physiology

entrain slow wave activity (Kelly & La Force, 1972; Sarna & Daniel, 1973; McCallum, 1987; Miedema *et al.* 1992). Pacing of the stomach has been used as a means to induce early satiety but has also been applied to reset regular slow-wave activity, and at higher frequencies, to restore normal gastric emptying and improve dyspeptic symptoms, such as nausea and vomiting (McCallum *et al.* 1998; Lin *et al.* 1998; Ladabaum & Hasler, 1999; Bortolotti, 2002). Although electrical pacing has been employed in animals and humans, the mechanism of slow wave phase advancement and the cells that transduce exogenous electrical currents have not been clearly identified. Previous studies have suggested that pacing of gastric muscles is mediated via ICC because slow waves cannot be evoked with exogenous current in gastric muscles lacking ICC (Ordog *et al.* 1999), and regenerative potentials (the response of ICC-IM/smooth muscle bundles) cannot be evoked in muscle bundles lacking ICC-IM (Suzuki *et al.* 2003). We have tested the hypothesis that ICC-IM are a critical link in enteric neural regulation of slow wave frequency. To test this hypothesis we have compared responses of wild-type and W/W^V mice to short pulse stimulation that exclusively activates intrinsic neurons, and longer pulse stimulation that can directly activate ICC-MY. W/W^V mice contain nearly normal populations of ICC-MY along the greater curvature of the antrum, but have no ICC-IM (Burns *et al.* 1996; Ordog *et al.* 2002; Hirst *et al.* 2002*a*); therefore tissues from these animals provide a means to directly test the importance of ICC-IM in mediating neural inputs and direct stimulation of the pacemaker apparatus.

METHODS

Animal treatment

BALB/c, W/W^V mutant mice and wild-type siblings (C57BL/6 +/+) between the ages 30 and 60 days were used for these studies. Animals were obtained from the Jackson Laboratory (Bar Harbor, MN, USA). Mice were anaesthetized with isoflurane (Baxter, Deerfield, IL, USA) prior to cervical dislocation and decapitation.

The animals were maintained and the experiments performed in accordance with the National Institutes of Health Guide for the Care and Use of Laboratory Animals, and the Institutional Animal Use and Care Committee at the University of Nevada approved all procedures used.

Electrophysiological experiments

After animals were killed, stomachs including approximately 5 mm of oesophagus and 10 mm of duodenum were removed and placed in Krebs–Ringer bicarbonate solution (KRB). The gastric antrum was isolated by a surgical incision across the stomach below the corpus and a second across the terminal antrum above the pylorus. The antrum was opened along the lesser curvature and gastric contents were washed away with KRB. The antrum was subsequently pinned to the base of a Sylgard silicone elastomer (Dow Corning Corp., Midland, MI, USA) dish and the mucosa was removed by sharp dissection. The entire terminal antrum (approximately 12 mm × 4 mm) was isolated and placed in a recording chamber with the serosal aspect of the muscle facing upward.

Impalements of cells were made with glass microelectrodes having resistances of 80–120 MΩ. Transmembrane potentials were recorded with a standard electrometer (Intra 767; World Precision Instruments, Sarasota, FL, USA). Data were recorded on digital tape (Vetter, Robersburg, PA, USA) or on a PC running AxoScope 8.0 data acquisition software (Axon Instruments, Union City, CA, USA) and hard copies were made by replaying the tapes through a polygraph (Gould RS 3200, Cleveland, OH, USA) or printed using Clampfit analysis software (Axon Instruments). All experiments were performed in the presence of nifedipine (1 μM) to reduce contractions and facilitate impalements of cells for extended periods. It has been previously demonstrated that slow waves in the murine antrum are not affected by nifedipine (Suzuki & Hirst, 1999). In all experiments, parallel platinum electrodes were placed on either side of the muscle strips and neural responses were elicited by square wave pulses of electrical field stimulation (EFS; 0.1–1.0 ms pulse duration, frequencies ranging between 1 and 30 Hz, train duration of 100–1000 ms, 10–15 V) using a Grass S48 stimulator (Quincy, MA, USA).

Solutions and drugs

The bath chamber was constantly perfused with oxygenated KRB of the following composition (mM): NaCl 118.5; KCl 4.5; $MgCl_2$ 1.2; $NaHCO_3$ 23.8; KH_2PO_4 1.2; dextrose 11.0; $CaCl_2$ 2.4. The pH of the KRB was 7.3–7.4 when bubbled with 97 % O_2–3 % CO_2 at 37 ± 0.5 °C. After pinning, the muscles were left to equilibrate for at least 1 h before experiments began. Nifedipine was obtained from Sigma (St Louis, MO, USA) and dissolved in ethanol at a stock concentration of 10 mM before being added to the perfusion solution at a final concentration of 1 μM. Atropine, apamin, N^{ω}-nitro-L-arginine (L-NA) and TTX were also obtained from Sigma and dissolved in de-ionized H_2O before being diluted in KRB to the final concentration.

Analysis of electrophysiological data

Data are expressed as means ± S.E.M. Student's *t* test and the Mann-Whitney rank sum test were used where appropriate to evaluate differences in the data. *P* values less than 0.05 were taken as a statistically significant difference. The '*n*' values reported in the text refer to the number of muscle strips used for each experimental protocol. Each muscle strip used in *n* values was taken from a separate animal. Several electrical parameters were analysed: (i) resting membrane potential (RMP); (ii) slow wave amplitude; (iii) duration of slow wave at half-maximal amplitude; (iv) the slow wave cycle period (SWCP), i.e. the time elapsed between the peak of the upstroke potential of two consecutive slow waves; and (v) frequency. Figures displayed were made from digitized data using Adobe Photoshop 4.0.1 (Adobe Co., Mountain View, CA, USA) and Corel Draw 7.0 (Corel Corp., Ontario, Canada).

Analysis of slow wave cycle period

In order to compare the regularity of slow wave frequency in wild-type *versus* W/W^V antrum muscles, we performed an analysis of slow wave cycle period (SWCP) variance for both animal groups. Fifteen slow waves recorded under control conditions were used to determine the pre-stimulus average SWCP. Standard deviation of the mean and variance were tabulated from this average for each animal. A Mann-Whitney rank sum test was performed to determine whether the SWCP variance values were statistically different in wild-type *versus* W/W^V animals.

Phase advancement analysis

For each animal, the SWCP of five spontaneous slow waves prior to EFS were measured to determine the 95 % confidence limits of

Journal of Physiology

the mean SWCP. To determine whether a slow wave could be prematurely evoked by EFS (0.1 and 1.0 ms pulses, delivered at frequencies ranging between 1 and 30 Hz) the SWCP between the slow wave immediately preceding EFS and that following stimulation was expressed as a percentage of the mean SWCP. If the SWCP between the slow wave prior to and after stimulation fell below the 95 % confidence limits of the mean spontaneous SWCP it was considered that the phase advancement was statistically significant.

Immunohistochemistry

Immunohistochemical analysis was performed on strips of terminal antrum muscles removed from the greater curvature of all three mice strains. Whole mount preparations were prepared after removing the mucosa by sharp dissection. The remaining strips of tunica muscularis were pinned to the base of a dish filled with Sylgard elastomer (Dow Corning Corp., Midland, MI, USA) with the circular muscle layer facing upward. Tissues were fixed in acetone (4 °C; 10 min). Following fixation, preparations were washed for 60 min in phosphate buffered saline (PBS; 0.01 M, pH 7.4). Incubation of tissues in 1 % bovine serum albumin for 1 h at room temperature containing 0.3 % Triton X-100 was used to reduce non-specific antibody binding. For examination of interstitial cells of Cajal, tissues were incubated overnight at 4 °C with a rat monoclonal antibody raised against Kit protein (ACK2;

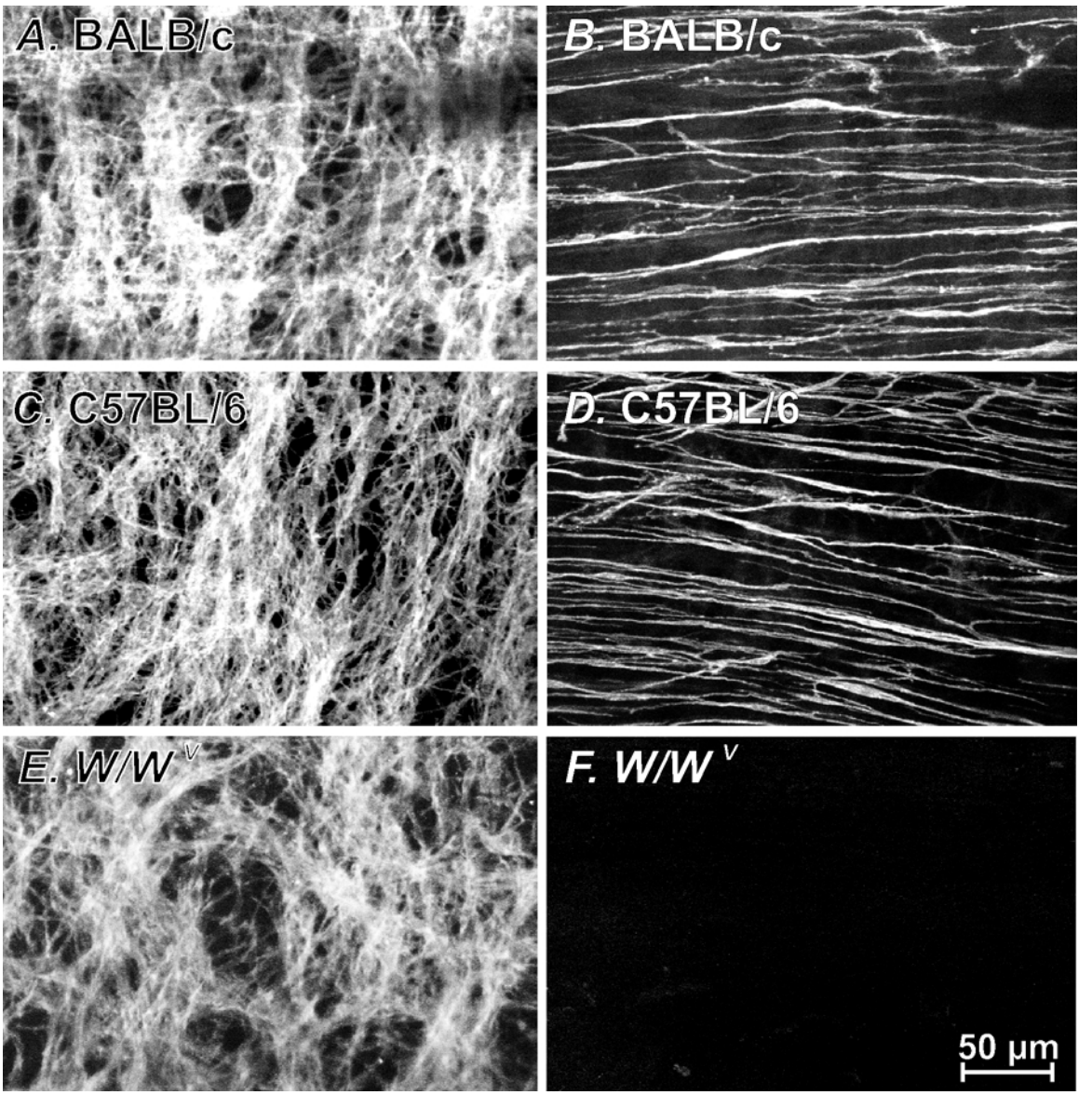

Figure 1. Kit-like immunohistochemistry revealed the distribution of specific classes of ICC in gastric antrum of BALB/c, C57BL/6 +/+ and *W/W^V* mice

The density of kit-immunopositive interstitial cells of Cajal (ICC) at the level of the myenteric plexus (ICC-MY) was greatest in the region of the greater curvature in BALB/c(*A*), C57BL/6+/+ (*C*) and *W/W^V* mice (*E*), as previously demonstrated (see Ordog *et al.* 2002; Hirst *et al.* 2002*a*). Spindle-shaped intramuscular ICC (ICC-IM) were distributed throughout the circular muscle layer and were in equal densities in both BALB/c and C57BL/6 wild-type mice (*B* and *D*). In contrast, ICC-IM were absent within the circular muscle layer of *W/W^V* animals (*F*).

Journal of Physiology

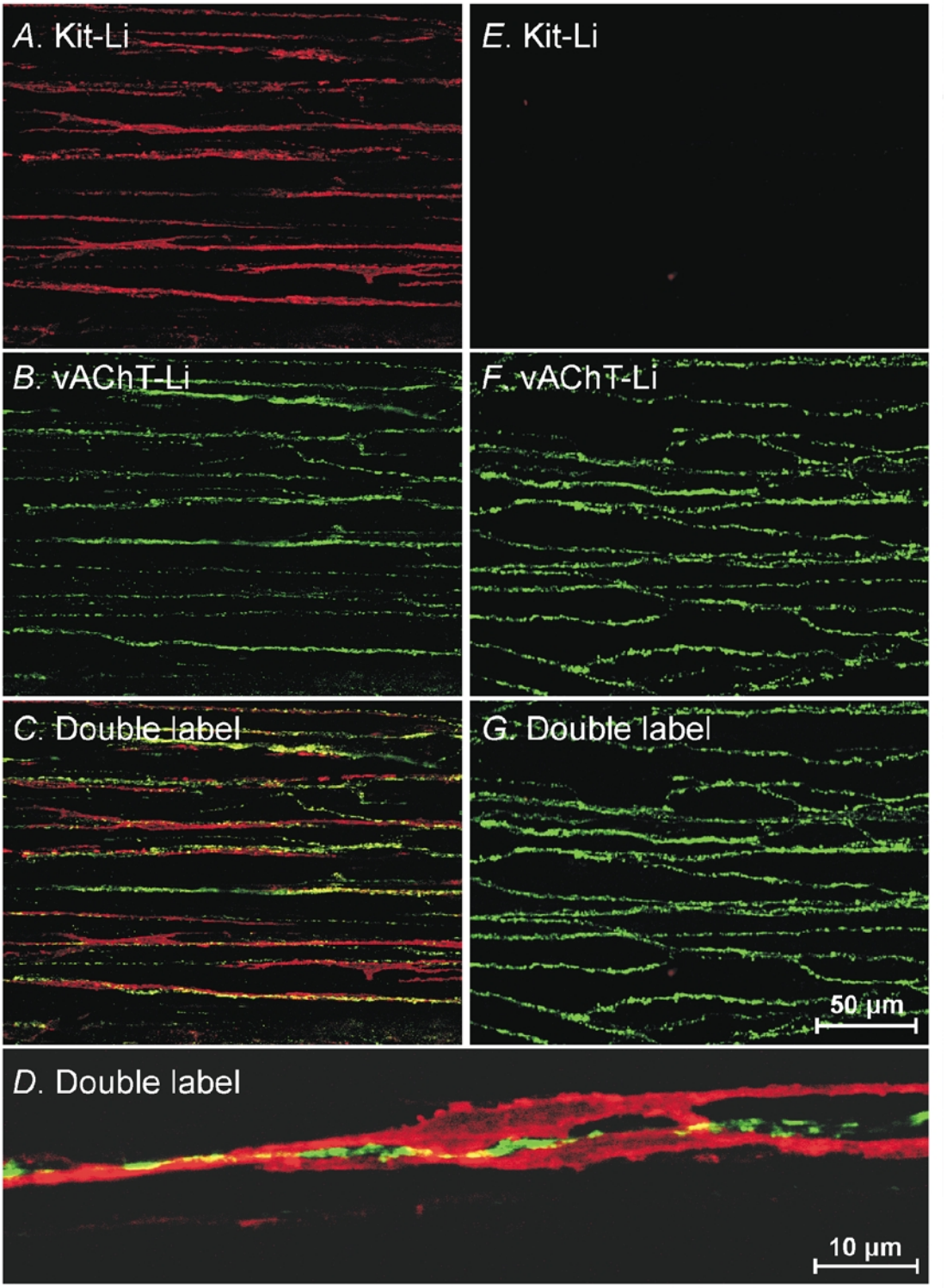

Figure 2. ICC-IM and intrinsic cholinergic motor nerves are closely apposed within the circular muscle layer of the gastric antrum

In wild-type animals, immunohistochemical labelling for Kit (Kit-Li; *A*; red) and vesicular acetylcholine transporter (vAChT-Li; *B*; green) revealed that nerve bundles containing vAChT-positive fibres were closely associated with ICC-IM (red). (*C*, overlay of micrographs *A* and *B*). A higher magnification of the close apposition between vAChT-Li nerves and ICC-IM is shown in *D*. Despite the absence of Kit-immunopositive ICC-IM in the circular muscle layer of W/W^{V} mutants (*E*), the distribution of vAChT-Li enteric motor nerves was similar to that of wild-type strains (*F*). (*G*, overlay of micrographs *E* and *F*).

Journal of Physiology

5 μg ml^{-1} in PBS; Gibco-BRL, Gaithersburg, MD, USA). Immunoreactivity was detected using fluorescein isothiocyanate-conjugated secondary antibody (FITC-anti rat; Vector Laboratories, Burlingame, CA, USA; 1:100 in PBS, 1 h, room temperature). Control tissues were prepared in a similar manner, omitting ACK2 from the incubation solution.

Tissues were examined with a Biorad MRC 600 (Hercules, CA, USA) confocal microscope with an excitation wavelength appropriate for FITC (488 nm). Confocal micrographs are digital composites of Z-series scans of 5–15 optical sections through a depth of 10–15 μm. Final images were constructed with Comos software (Bio-Rad, Hercules, CA, USA).

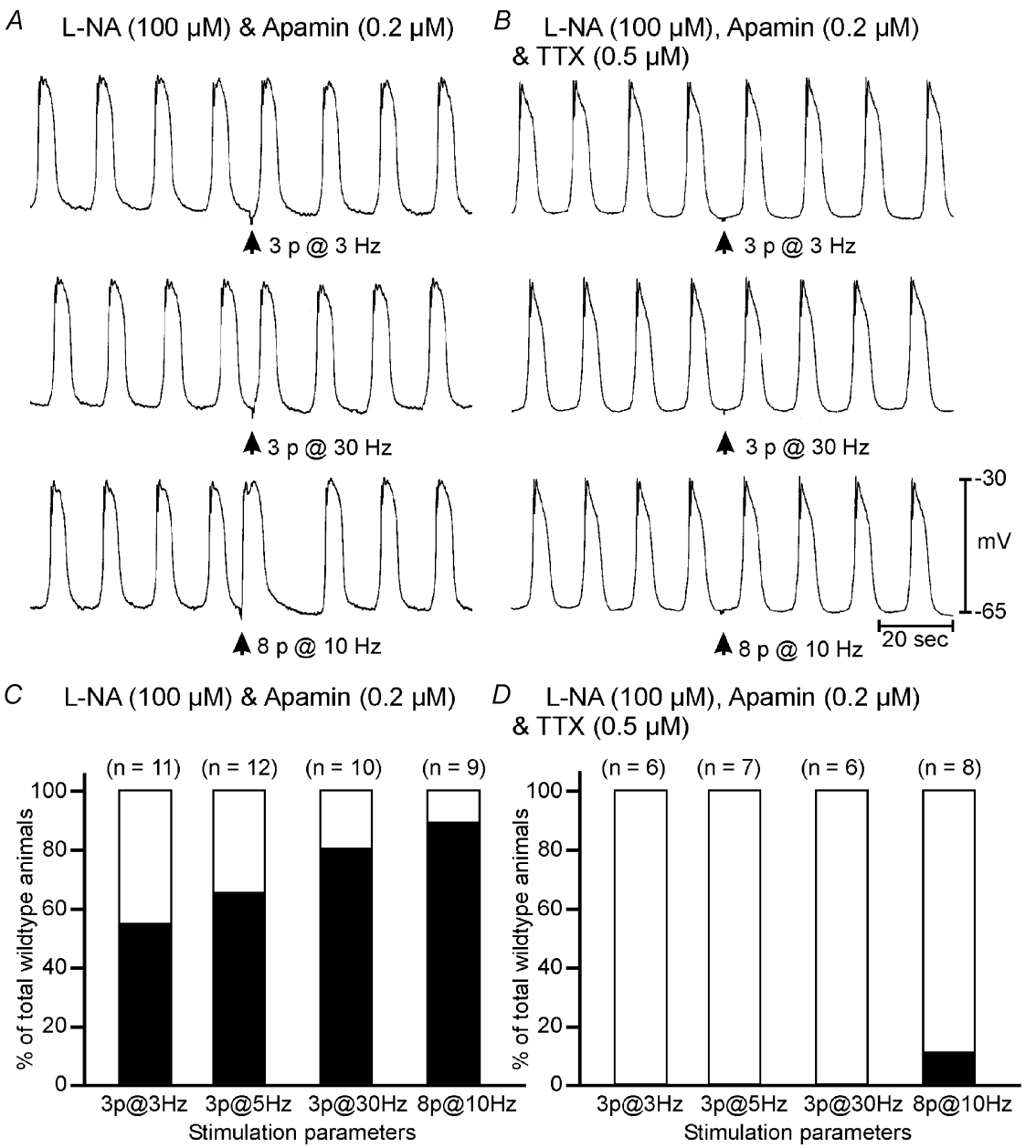

Figure 3. Slow wave events can be phase advanced by short duration (0.1 ms) pulses of electrical field stimulation (EFS) in wild-type antrum muscles

A, in the presence of N^{ω}-nitro-L-arginine (L-NA) (100 μM) and apamin (0.2 μM) slow wave events were prematurely evoked by trains of short duration pulses (0.1 ms; 3–8 pulses at frequencies of 3–30 Hz; delivered at arrows). *B*, tetrodotoxin (0.5 μM) abolished the phase advancement of slow waves. *C*, summarized data from wild-type animals reveals that the advancement of slow wave events in the presence of L-NA and apamin was frequency dependent. As stimulation frequency was increased the percentage of animals in which phase advancement occurred increased (i.e. 54 % of wild-type animals showed phase advancement with 3 pulses at 3 Hz, whereas 80 % showed phase advancement with 3 pulses at 30 Hz (*C*)). In the presence of TTX (0.5 μM), slow waves could not be phase advanced at any frequency except in one tissue at a stimulus parameter of 8 pulses at 10 Hz (*D*). Scale bars at the bottom of *B* apply to all panels.

Journal of Physiology

RESULTS

Distribution of ICC in wild-type and W/W^V gastric antrum

Kit-like immunoreactivity revealed the distribution and density of specific classes of ICC in the murine gastric antrum. ICC at the level of the myenteric plexus (ICC-MY) had the greatest density along the greater curvature of the antrum. There were no obvious differences in the distribution or density of ICC between control mice strains within this region of the antrum (i.e. between wild-type and BALB/c mice; Fig. 1*A* and *C*). In W/W^V mice ICC-MY along the greater curvature of the terminal antrum were of approximately the same density as in control animals (Fig. 1*E*), as previously quantified (Ordog *et al.* 2002).

Kit-like immunoreactivity revealed intramuscular ICC (ICC-IM) within the circular muscle layer of wild-type and BALB/c gastric antral muscles. These cells possessed a spindle-shaped morphology and were interposed between and ran parallel to the smooth muscle fibres (Figs 1*B*, 1*D* and 2*A*). ICC-IM were absent in W/W^V mutants (Figs 1*F* and 2*E*).

Close morphological relationship between cholinergic motor nerves and ICC-IM within the antral circular muscle layer

Antibodies directed against the vesicular acetylcholine transporter (vAChT) revealed varicose nerve fibres within the circular muscle layer of wild-type (C57BL/6 +/+) animals. These fibres ran parallel to the circular smooth muscle cells (Fig. 2*B*). The density of innervation of vAChT-immunopositive nerve fibres was 33.6 ± 4.6 per 10^{-3} mm^3 (cube volume with dimensions of 100 × 100 × 100 μm) within the circular muscle layer of wild-type tissues (n = 14 composite images from three wild-type (C57BL/6 +/+) animals; images taken from greater curvature of terminal antrum; Fig. 2*B*). Double labelling for vAChT and Kit in wild-type controls revealed that varicose nerve fibres containing vAChT were closely apposed to ICC-IM (Fig. 2*C* and *D*) and frequently remained in close contact for distances greater than 200 μm. The density of ICC-IM within the circular muscle layer at the greater curvature was 33.9 ± 5.5 per 10^{-3} mm^3 which was not significantly different from the density of vAChT-immunopositive fibres within the same region (n = 14 composite images from three wild-type animals; $P > 0.5$ compared with density of vAChT-Li nerve fibres). Occasional vAChT-immunopositive nerve fibres were observed to be closely apposed to more than one ICC-IM. Double labelling W/W^V gastric antrum tissues with vAChT-Li and Kit-Li revealed that despite the absence of ICC-IM (Fig. 2*E*), vAChT-Li nerve fibres were present within the circular layer and had an average density that was similar to wild-type controls (48.9 ± 3.8 fibres per 10^{-3} mm^3; n = 15 composite images taken from three W/W^V animals; Fig. 2*F* and *G*).

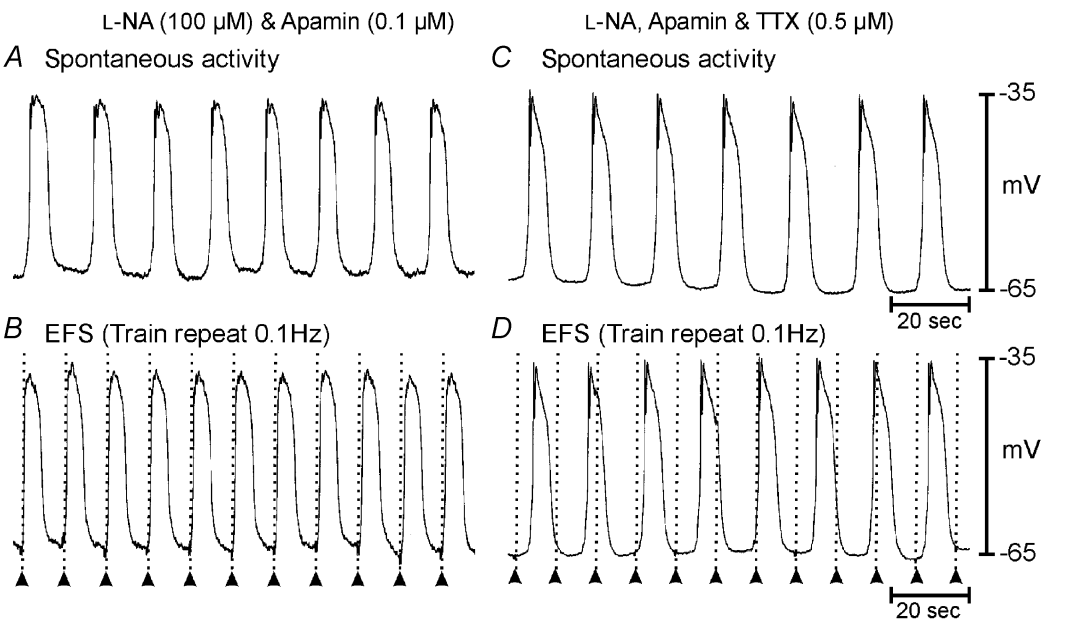

Figure 4. Slow waves can be paced by short duration (0.1 ms) pulses of EFS in wild-type antrum muscles

A, in the presence of L-NA (100 μM) and apamin (0.2 μM) slow waves occurred spontaneously at a frequency of 0.07 Hz (4.4 cycles min^{-1}). *B*, trains of short duration pulses (0.1 ms; 3 pulses at 5 Hz; supra-optimal voltage) delivered at a frequency of 0.1 Hz entrained slow waves at a rate of 6 cycles min^{-1}. Application of tetrodotoxin (TTX; 0.5 μM) did not alter spontaneous slow wave frequency (*C*) but inhibited electrical entrainment of slow waves (*D*). Time scale bars are indicated in panels *C* and *D*.

Journal of Physiology

Characteristics of spontaneous electrical slow wave activity in the murine gastric antrum

Spontaneous rhythmic depolarizations (slow waves) were recorded from circular smooth muscle cells at an average frequency of 4.5 cycles min^{-1}, which is similar to previous recordings from this region of the murine stomach (Kim *et al.* 2002). Antral slow waves are largest at the greater curvature of the antrum because this region of the antrum has the highest density of ICC-MY pacemaker cells (Ordog *et al.* 2002; Hirst *et al.* 2002*a*). Therefore in the present study all slow waves were recorded from the circular muscle layer of the terminal antrum in the region of the greater curvature. Slow waves in this region consisted of an initial rapid depolarization, followed by partial repolarization to a plateau phase that was maintained for several seconds before cells repolarized to the diastolic membrane potential (resting membrane potential; RMP). In some tissues (e.g. see Figs 7, 10 and 11) oscillations in membrane potential occurred during the plateau phase of slow waves. These events occurred in the presence of nifedipine (1 μM) and thus were not due to Ca^{2+} action potentials. In some cases the initial depolarization was associated with an increase in electrical noise and a small inflection during the upstroke depolarization (see Dickens *et al.* 1999 for explanation of this feature).

In BALB/c mice and wild-type siblings of W/W^V mutants (C57BL/6 +/+) slow waves averaged 27.3 ± 1.3 mV in amplitude, occurred at a frequency of 4.5 ± 0.2 cycles min^{-1}, and had an average half-maximal duration of 4.2 ± 0.2 s. The slow wave cycle period, measured between the peak of the upstroke potential of two consecutive slow waves, averaged 13.5 ± 0.8 s in duration (n = 27). There was no statistical difference in any of these parameters between BALB/c and C57BL/6 +/+ mice (n = 16 for BALB/c and n = 11 for C57BL/6 +/+ mice; $P > 0.05$ for all parameters).

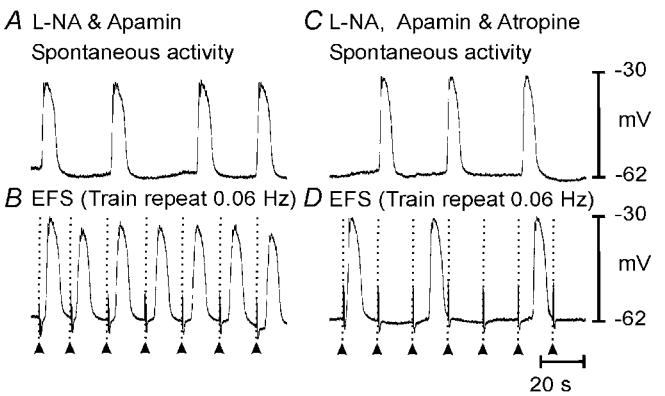

Figure 5. Blockade of muscarinic receptors prevents gastric antrum entrainment

Spontaneous slow waves recorded from the greater curvature of the terminal antrum (*A*) could be paced up to twice the intrinsic rate using trains of EFS (0.1 ms pulse duration; 3 pulses at 5 Hz; supra-optimal voltage) (*B*). Atropine (1 μM) did not significantly alter spontaneous slow wave frequency (*C*) but prevented slow wave entrainment at higher frequencies (*D*). Timescale bar shown in *D* is the same for all panels.

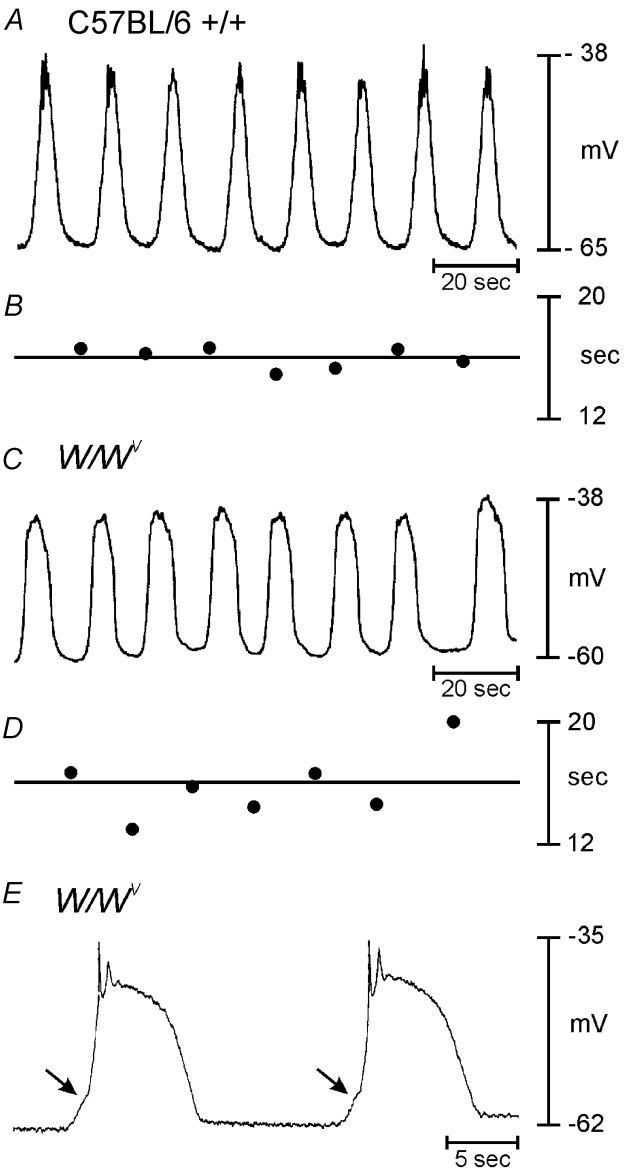

Figure 6. The slow wave cycle period was more variable in W/W^V animals than their wild-type siblings

A, slow waves recorded from the terminal antrum of a C57BL/6 wild-type control animal. The straight line in *B* represents the mean slow wave cycle period (SWCP) calculated from 15 consecutive slow waves. From cycle to cycle, individual SWCPs (represented by filled circles) varied around a mean of 16 s (*B*). *C*, discharge of slow waves from the terminal antrum of W/W^V animals was generally more irregular. *D*, demonstration of the variance of individual SWCPs (filled circles) from the mean SWCP value (continuous line). *E*, examination of W/W^V slow waves on an expanded time scale reveals two components to the slow waves as previously described in murine antral muscles (e.g. Dickens *et al.* 2001); arrows denote inflection in upstroke potential separating the 1st and 2nd components.

Phase advancement of slow waves using short-duration pulses

Electrical field stimulation (EFS; 0.1 ms duration) was applied to antrum muscles during the diastolic period between slow waves. To determine if phase advancement of slow waves occurred, the slow wave cycle period (SWCP) for five spontaneous events prior to EFS was compared with the SWCP of events occurring immediately prior to and following EFS. Several stimulation parameters were utilized ranging from a single pulse (0.1 ms in duration) to a series of three pulses (each 0.1 ms) delivered at frequencies of 3, 5, 10, 20 and 30 Hz. Experiments were performed under control conditions and after the addition of specific neuronal antagonists.

Under control conditions EFS produced a frequency-dependent hyperpolarization in membrane potential

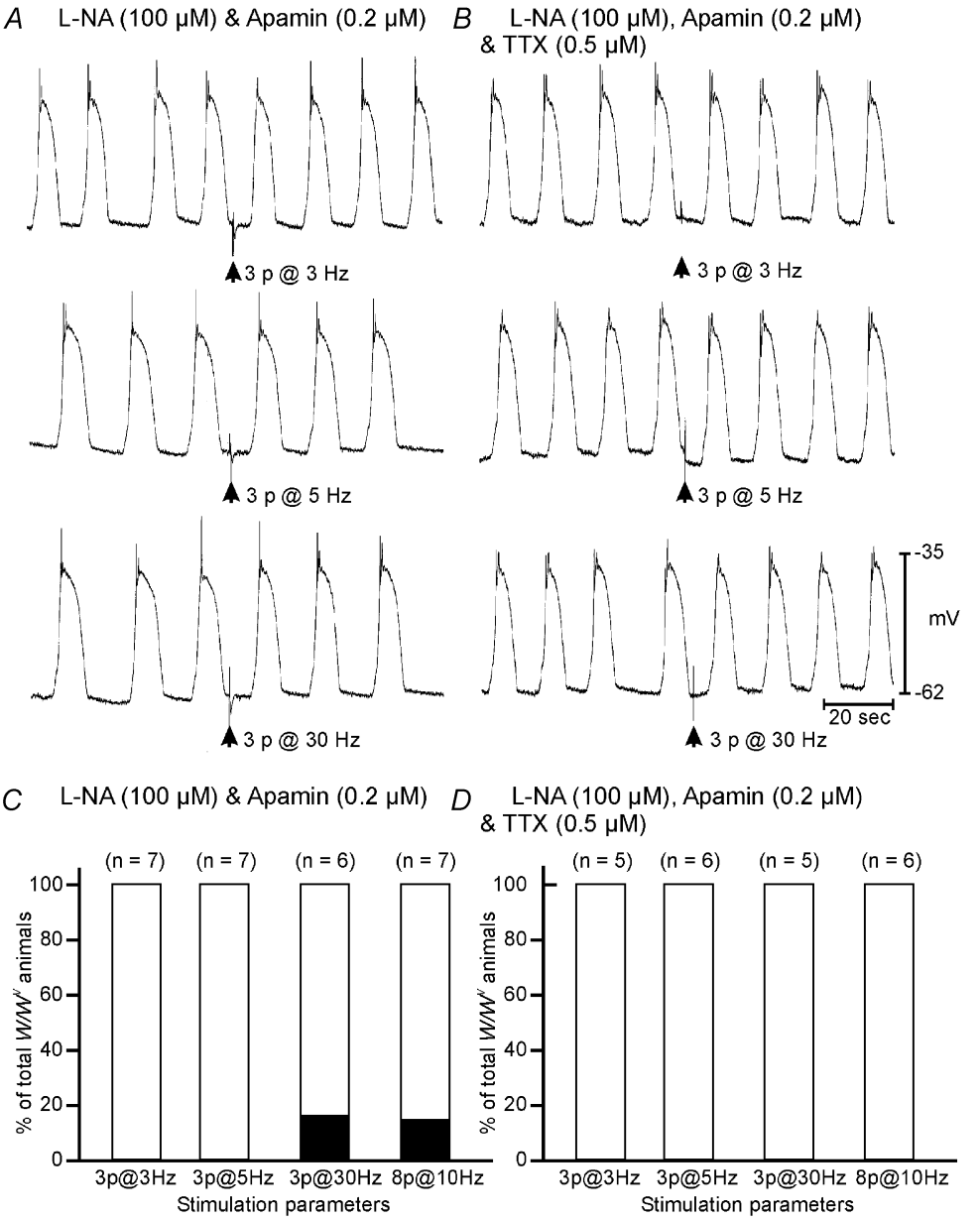

Figure 7. Short duration (0.1 ms) pulses of EFS fail to elicit premature slow wave events in *W/W^V^* antrum muscles

A, in the presence of L-NA (100 μM) and apamin (0.2 μM) slow waves from a W/W^V antrum could not be phase advanced using 0.1 ms duration pulses of EFS delivered at frequencies of between 3 and 30 Hz. *B*, TTX did not alter the response to EFS. *C*, summarized data from all W/W^V animals shows that failure of phase advancement was consistent, with only one W/W^V antrum tissue showing statistical phase advancement following high frequency stimulation (3 pulses at 30 Hz and 8 pulses at 10 Hz). *D*, in the presence of TTX, slow waves could not be phase advanced at any frequency in W/W^V animals. Scale bars at the bottom of *B* apply to all panels.

Journal of Physiology

(inhibitory junction potential or IJP) and in approximately 50 % of tissues it caused phase advancement of slow wave activity. In order to avoid the influences of inhibitory neurotransmitters all other experiments were performed in the presence of N^{ω}-nitro-L-arginine (L-NA; 100 μM), an inhibitor of nitric oxide synthase (NOS), and apamin (0.2 μM), a blocker of small conductance K^+ channels that are activated post-junctionally in response to release of ATP (Banks *et al.* 1979; Vogalis & Goyal, 1997; Koh *et al.* 1997)

In the presence of L-NA and apamin, the phase advancement of slow waves immediately following EFS was enhanced with all stimulation parameters tested (Fig. 3*A*). The effects of EFS on the SWCP were analysed. The phase advancement of slow waves was frequency dependent, i.e. with three pulses at 3 Hz, phase advancement occurred in six out of eleven tissues, whereas with eight pulses at 10 Hz, phase advancement occurred in eight out of nine wild-type tissues (Fig. 3*C*). Application of tetrodotoxin (TTX, 0.5 μM) inhibited the phase advancement of slow waves at all frequencies tested except in one tissue at a stimulus parameter of eight pulses at 10 Hz (n = 8 animals; Fig. 3*B* and *D*). This suggests that the mechanism underlying the phase advancement of slow waves in response to short duration pulses of EFS was due to activation of enteric neurons.

Slow wave entrainment

As stated above the average spontaneous slow wave frequency averaged 4.5 cycles min^{-1} and had an average half-maximal duration of 4.2 s. The demonstration that EFS could phase advance slow waves suggested that it might be possible to increase or decrease the frequency of slow waves using EFS. Therefore we performed a series of experiments where EFS was delivered in short trains (0.1 ms pulse duration, 3–30 Hz) at a rate of 0.06–0.15 Hz, after spontaneous slow wave activity was recorded. This series of experiments was also performed in the presence of L-NA and apamin to remove the influences of inhibitory neurotransmitters. EFS delivered under these conditions produced a series of slow waves that could be entrained at the frequency of the EFS (Fig. 4*B*). There was variability in the rate at which antral muscles could be paced. For example, slow waves that had a low intrinsic frequency of 0.033 Hz (2 cycles min^{-1}) could not be paced greater than 0.07 Hz (4.2 cycles min^{-1}). While muscles with a higher intrinsic frequency of 0.092 Hz (5.5 cycles min^{-1}) could be

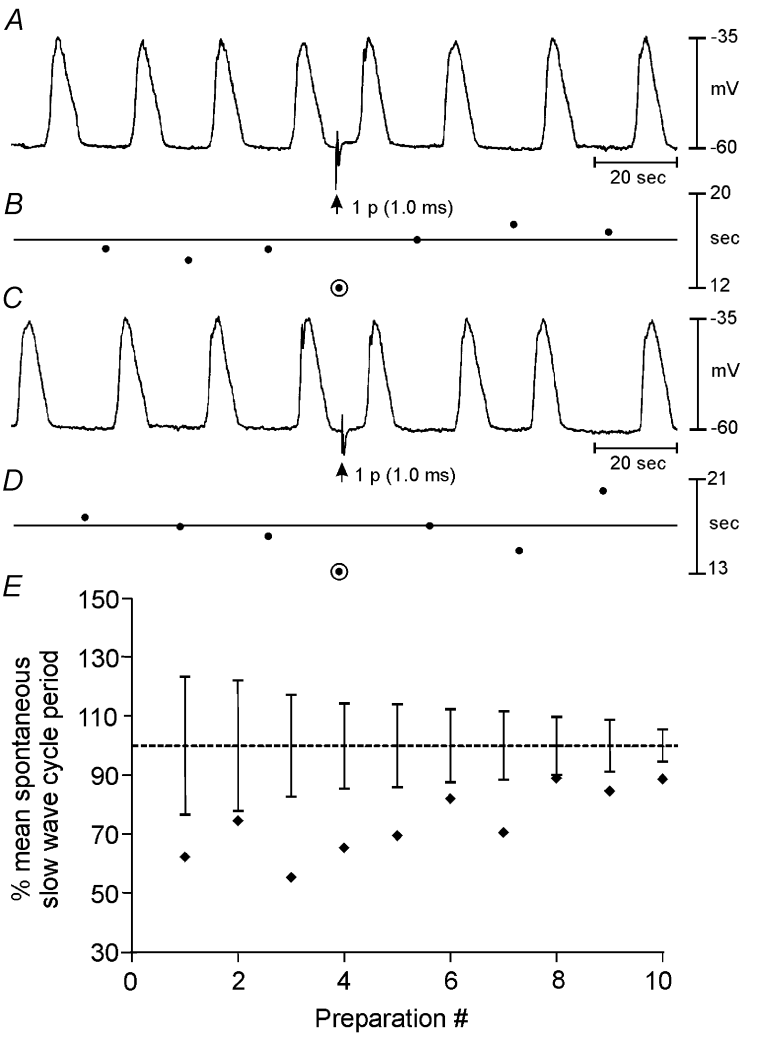

Figure 8. Phase advancement of slow waves using long duration pulses of EFS (1–2 ms pulse duration) does not require intrinsic nerve activation

A, in the presence of L-NA (100 μM) and atropine (1 μM) single 1.0 ms duration pulses of EFS (delivered at arrow) evoked premature slow wave events. *B*, slow wave cycle periods (SWCPs) between consecutive slow waves varied from cycle to cycle around a mean value of 16 s. The SWCP between the slow wave immediately preceding EFS and that following stimulation was significantly shorter than the mean SWCP by 12 s (depicted by the encircled filled circle in *B*). *C* and *D*, slow wave advancement in the presence of L-NA, atropine and TTX (0.3 μM). The remaining voltage transient is a stimulus artifact. *E*, summary of data from 10 wild-type animals. For each animal, the SWCP of five spontaneous slow waves prior to electrical field stimulation were measured to determine the 95 % confidence limits of the mean SWCP. The mean SWCP was expressed as 100 % and is represented by the dashed line. Each of the 10 vertical lines represents the 95 % confidence intervals of the mean SWCP for an individual animal. The SWCP between the slow wave immediately preceding EFS and that following stimulation was expressed as a percentage of the mean SWCP (filled diamonds). If this value fell below the 95 % confidence limits of the mean SWCP it was considered that phase advancement had occurred. In all 10 wild-type animals single 1.0–2.0 ms pulses of EFS produced phase advancement of the next slow wave in the presence of L-NA, atropine and TTX (*E*).

paced up to 0.15 Hz (9.0 cycles min^{-1}). We were unable to entrain slow waves at frequencies greater than 0.15 Hz (9.0 cycles min^{-1}). Termination of EFS caused slow waves to return to the intrinsic frequency within 5 min. In order to determine if the slow wave entrainment was neuronally mediated, experiments were performed in the presence of tetrodotoxin (TTX; 0.5 μM). TTX completely blocked the entrainment of slow waves that was observed under control conditions (Fig. 4*D*). Activation of cholinergic nerves contributed to the entrainment of slow waves because atropine (1 μM) also blocked the entrainment of slow wave activity (Fig. 5*D*).

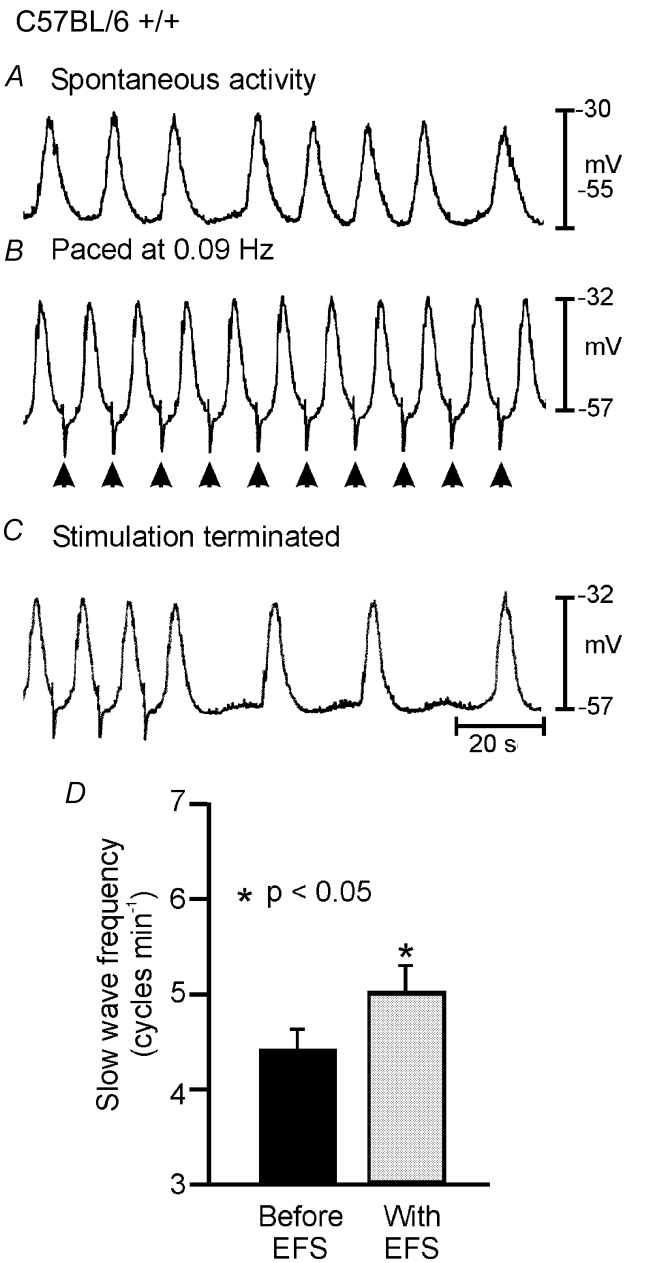

Figure 9. Longer duration pulses of EFS (1.0–2.0 ms) produced entrainment of slow waves in wild-type antrum muscles

In the presence of L-NA (100 μM), atropine (1 μM) and TTX (0.5 μM) spontaneous slow waves which discharged at an intrinsic rate of 0.067 Hz (4 cycles min^{-1}; *A*) could be entrained at 0.09 Hz (5.4 cycles min^{-1}; *B*) by single 1.0 ms pulses of EFS (supra-optimal voltage). *C*, the slow wave frequency returned to its intrinsic rate within 1 min after EFS was terminated. *D*, summary of data from wild-type entrainment experiments. The mean slow wave frequency for wild-type animals was 4.4 ± 0.2 cycles min^{-1} (black bar; n = 12) and this was increased using single pulse EFS (1.0–2.0 ms pulse duration) to a mean value of 5.0 ± 0.3 cycles min^{-1} (grey bar).

Role of ICC-IM in phase advancement and entrainment of slow waves

It has been reported that ICC-IM play a critical role in excitatory and inhibitory motor neurotransmission in the murine fundus (Burns *et al.* 1996; Ward *et al.* 2000*a*; Beckett *et al.* 2002). A similar role for these cells has also been recently reported in the gastric antrum (Hirst *et al.* 2002*c*; Suzuki *et al.* 2003). In order to determine the role of ICC-IM in the phase advancement and entrainment of slow waves we performed a series of experiments on the antral muscles of W/W^V mutant animals where ICC-IM are absent (see Figs 1*F* and 2*E*).

In W/W^V animals, slow waves recorded along the greater curvature of the antrum averaged 19.8 ± 1.7 mV in amplitude, which was significantly different from C57BL/6 and BALB/c animals (27.3 ± 1.3 mV; $P < 0.05$; n = 22 for C57BL/6). Despite this reduction in amplitude, slow waves occurred at a frequency of 4.8 ± 0.3 cycles min^{-1} and had an average half-maximal duration of 4.1 ± 0.2 s, which were not significantly different than wild-type animals ($P > 0.05$). The slow wave cycle period between consecutive slow waves averaged 13.2 ± 1.2 s in duration, which was similar to the average SWCP for wild-type animals (13.5 ± 0.8 s). However, slow wave frequency in individual W/W^V mutants was more variable than that of control animals (Fig. 6*A*–*D*). The mean variance of slow wave cycle period for W/W^V animals was 4.95 ± 1.14 s^2, which was significantly greater than for wild-type and BALB/c animals (1.37 ± 0.39 s^2; $P = 0.007$; n = 22 for C57BL/6 and BALB/c animals, n = 18 for W/W^V animals for all slow wave parameters).

It has been reported in guinea-pig and murine antral tissues that slow waves consist of two components (Dickens *et al.* 1999). The first component is thought to represent the electronic spread of pacemaker potentials generated by the dominant ICC-MY networks whereas the secondary component is thought to be generated by a summation of unitary potentials generated in ICC-IM (Hirst *et al.* 2002*c*). In the absence of ICC-IM (i.e. in W/W^V mutants) slow waves recorded from the greater curvature displayed two component slow waves (Fig. 6*E*). These data suggest that the secondary component of slow waves may be generated in the absence of ICC-IM.

Under control conditions, EFS (0.1 ms duration; 3–8 pulses at 3–30 Hz) delivered after a spontaneous slow wave

Journal of Physiology

did not phase advance the next slow wave in W/W^V animals. For all stimulation frequencies tested, the SWCP between the slow wave before and after EFS did not fall below the 95 % confidence limits of the mean SWCP. In the presence of L-NA (100 μM) and apamin (0.2 μM), EFS did not produce phase advancement in slow waves in W/W^V mutant animals using EFS with pulses 0.1 ms in duration and at frequencies between 3–30 Hz (Fig. 7*A* and *C*). TTX or atropine did not alter the response to EFS in W/W^V mutant animals (Fig. 7*B* and *D*).

To determine whether slow waves in W/W^V mutants could be entrained we applied EFS (0.1 ms duration) at the frequencies tested on wild-type muscles. Under control conditions and in the presence of L-NA and apamin, EFS at the parameters tested on wild-type muscles did not entrain slow waves (data not shown).

Direct stimulation of ICC-MY

In wild-type animals (C57BL/6 +/+ and BALB/c mice), in the presence of L-NA (100 μM) and atropine (1 μM), longer pulses of EFS (1.0–2.0 ms) produced a small apamin-sensitive (0.2 μM) inhibitory junction potential (data not shown). Despite the presence of L-NA and atropine, 1.0–2.0 ms duration EFS produced a phase advancement of the next slow wave event (Fig. 8*A* and *B*). TTX (0.5 μM) inhibited remaining non-nitrergic (apamin-sensitive) components of the IJP, when present, but did not prevent phase advancement of slow waves with 1.0–2.0 ms duration EFS (Fig. 8*C* and *D*). In the continued presence of L-NA, atropine and TTX, slow waves were entrained from an average intrinsic rate of 0.073 Hz (4.4 ± 0.2 cycles min^{-1}) to 0.087 Hz (5.0 ± 0.3 cycles min^{-1}; $n = 12$), suggesting that responses to these stimulation parameters were not neurally mediated (Fig. 9*A*–*C* and summarized in Fig. 9*D*).

Stimulating the antrum of W/W^V animals in the presence of L-NA (100 μM) and atropine (1 μM) using 1.0 ms duration pulses produced a large IJP and a phase advancement of the next slow wave (Fig. 10*A* and *B*). TTX blocked the IJP evoked by EFS but did not inhibit the phase advancement of slow waves following EFS (Fig. 10*C* and *D* and summarized in Fig. 10*E*). Slow waves were entrained

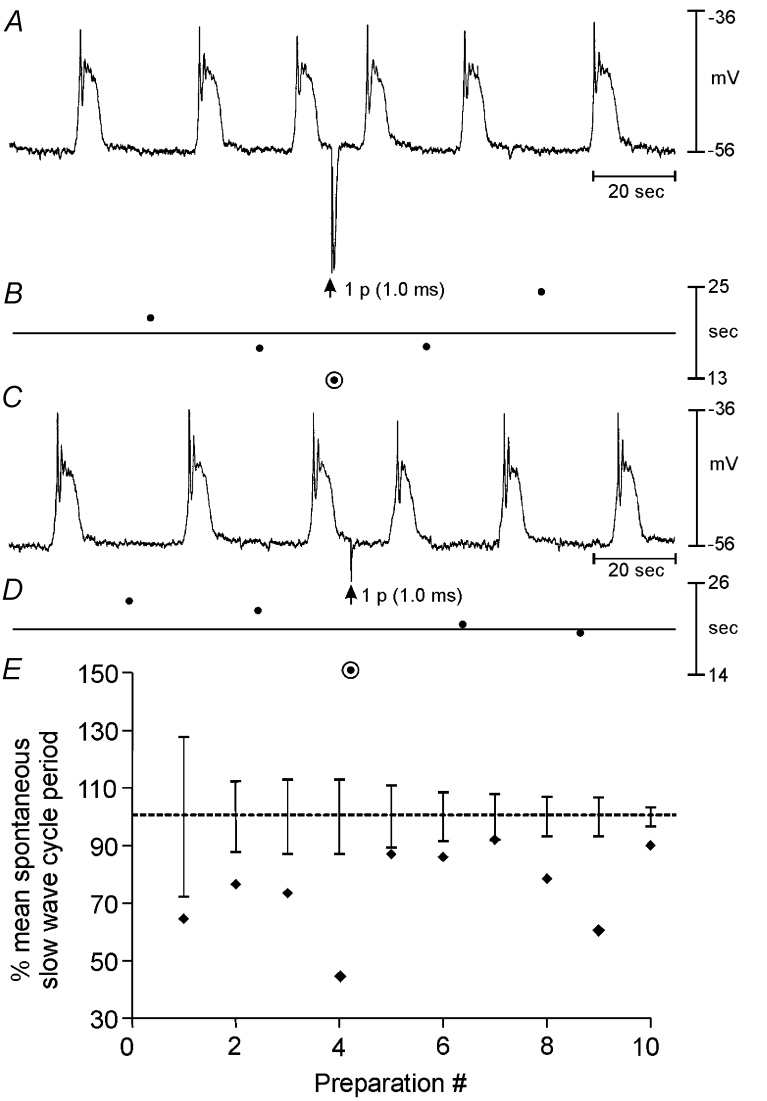

Figure 10. Slow waves in W/W^V antrum muscles can be phase advanced using longer duration pulses of EFS (1–2 ms pulse duration)

A, in the presence of L-NA (100 μM) and atropine (1 μM) single 1.0 ms duration pulses of EFS (delivered at arrow) evoked fast inhibitory junction potentials and premature slow wave events. *B*, individual slow wave cycle periods (SWCPs) varied from cycle to cycle around a mean value of 19 s. The SWCP between the slow wave immediately preceding EFS and that following stimulation was 14 s significantly shorter than the mean SWCP (depicted by the encircled filled circle in *B*). *C* and *D*, TTX blocked the large inhibitory junction potential evoked by EFS but did not inhibit the phase advancement of slow waves following EFS. *E*, summary of data from 10 W/W^V animals, analysed as described for Fig. 8. In 9 out of 10 W/W^V animals the SWCP between the slow wave immediately preceding EFS and that following stimulation fell below the 95 % confidence limits of the mean SWCP, indicating that phase advancement had occurred (*E*).

Journal of Physiology

in the presence of L-NA (100 μM), atropine (1 μM) and TTX (0.5 μM) using 1.0–2.0 ms EFS from an intrinsic rate of 4.9 ± 0.5 to 6.5 ± 0.6 cycles min^{-1} (n = 9; Fig. 11*A–C* and summarized in Fig. 11*D*), suggesting that activation of intrinsic nerves was not required for this response. Activation of premature slow waves by single pulses of EFS with durations in the order of 1.0–2.0 ms in W/W^V mutants (that lack ICC-IM) suggest that in these muscles EFS may directly activate ICC-MY.

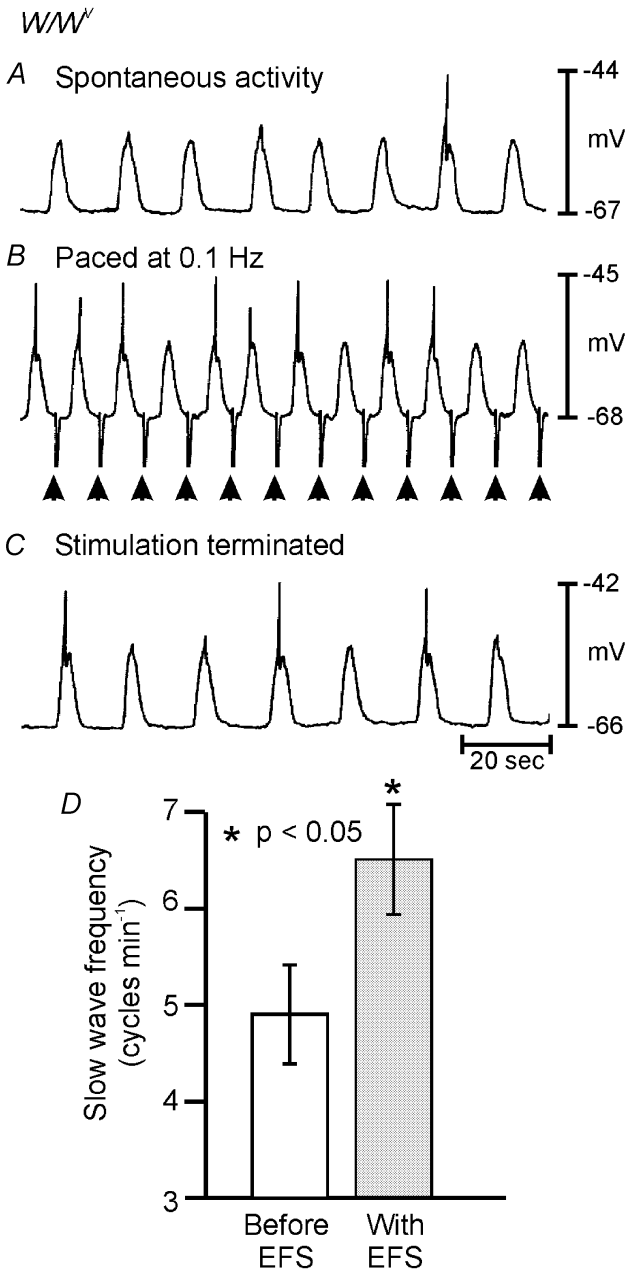

Figure 11. Entrainment of W/W^V antral slow waves using single 1.0–2.0 ms pulses of EFS

Spontaneous slow waves occurring at a rate of 4 cycles min^{-1} (0.067 Hz; *A*) were entrained at a frequency of 6 cycles min^{-1} (0.1 Hz; *B*) by single pulses of EFS (1.0 ms; supra-optimal voltage; delivered at arrows). *C*, slow wave discharge returned to the intrinsic frequency of 0.067 Hz soon after termination of EFS. *D*, summary of data from W/W^V entrainment experiments. The mean intrinsic frequency of slow wave discharge from W/W^V animals was 4.9 ± 0.5 cycles min^{-1} (open bar) and was increased to 6.5 ± 0.6 cycles min^{-1} using 1.0–2.0 ms EFS (grey bar; n = 9). Entrainment experiments using 1.0–2.0 ms pulses of EFS were performed in the presence of L-NA (100 μM), atropine (1 μM) and TTX (0.3 μM).

DISCUSSION

Slow waves in the stomach originate from ICC-MY and conduct passively (i.e. with decrement) into smooth muscle cells (Dickens *et al.* 1999; Ordog *et al.* 1999). The depolarization response to slow waves in smooth muscle cells determines the amount of Ca^{2+} entry and the force of gastric peristaltic contractions (Ozaki *et al.* 1991). An important part of the regulation of the smooth muscle response to slow wave depolarization comes from the action of intrinsic excitatory and inhibitory motor neurons. In the present study we found that neural regulation of slow wave frequency was lost in W/W^V mice that lack ICC within muscle layers (ICC-IM and ICC-SEP). Our observations support the hypothesis that neural regulation of slow wave frequency is mediated through ICC-IM and/or ICC-SEP. In wild-type animals, slow waves could be phase advanced by cholinergic stimulation and repetitive stimulation was capable of entraining slow waves at a rate higher than the intrinsic frequency. These data are complementary with the recent finding that cholinergic neurons can activate cells within muscle bundles of the guinea-pig antrum and drive the pacemaker apparatus (Hirst *et al.* 2002*c*). TTX- or atropine-sensitive phase advancement and entrainment of slow waves at higher frequencies did not occur in W/W^V animals in the absence of ICC-IM and ICC-SEP. Taken together, these data demonstrate the critical role of ICC-IM in gastric muscles. These cells mediate neural inputs, and, by conduction of depolarizing currents into the electrically coupled ICC-MY network (Hirst *et al.* 2002*c*), mediate neural regulation of slow wave frequency. Regulation of slow wave frequency is a fundamental issue in GI motility that directly impacts gastric peristaltic contractions.

Previous studies have shown that slow waves could not be elicited by EFS in murine antral muscles made devoid of ICC by treatment with Kit-neutralizing antibodies (Ordog *et al.* 1999). Antral muscles of W/W^V mice, which lack ICC-IM, could be paced with 1–2 ms duration pulses, suggesting that although ICC-IM are critical for neurally evoked responses, they are not required for the direct electrical stimulation of ICC-MY. These data, coupled with the general observations that smooth muscle cells have membrane time constants of 50–150 ms (Tomita, 1981) and do not express the ionic mechanisms necessary to generate slow waves (Horowitz *et al.* 1999), suggest that activation of smooth muscle cells is not responsible for direct activation (i.e. non-neural pacing) of gastric

Journal of Physiology

muscles of W/W^V mice. These data provide evidence that the primary pacemaker mechanism in ICC-MY can be activated directly by extrinsic currents that are too short in duration to elicit responses in smooth muscle cells.

The experiments we have performed raise questions about how neural (cholinergic) inputs and direct current stimulation activate premature slow waves in ICC. The model of slow wave generation (and regenerative potential generation in ICC-IM/smooth muscle bundles; see Edwards *et al.* 1999) favoured by most investigators is that slow wave and regenerative potentials are initiated by Ca^{2+} release from inositol 1,4,5-trisphosphate (IP_3) receptor-operated stores (Suzuki & Hirst, 1999; Van Helden *et al.* 2000; Ward *et al.* 2000*b*). Stimulation of cholinergic nerves and activation of post-junctional M3 receptors (which are expressed in GI muscles and ICC-IM; see Epperson *et al.* 2000) would be expected to activate phospholipase C $(PLC)_\beta$ (Gq/G11 coupled) and enhance production of IP_3. This would accelerate the IP_3 receptor-operated release of Ca^{2+} and tend to phase advance slow wave events. Activation of ICC-MY either by the conduction of regenerative potentials from ICC-IM (in wild-type mice) or by direct stimulation by exogenous current (in wild-type and W/W^V mice lacking ICC-IM) is more controversial. Nose and coworkers proposed that current stimulation activates premature slow waves or regenerative potentials by voltage-dependent enhanced synthesis of IP_3, quoting studies suggesting a voltage-sensor in PLC couples depolarization to IP_3 synthesis (Nose *et al.* 2000; Mahaut-Smith *et al.* 1999). Mahaut-Smith and co-workers (1999) have demonstrated voltage-dependent synthesis of IP_3 in response to long duration depolarizations. We have shown premature initiation of slow waves by pulses of 1 ms duration. Thus, extremely brief depolarization affects the slow wave initiation mechanism. Since IP_3 production has never been shown to occur in response to such brief depolarization, we would suggest that rather than IP_3 synthesis under the direct control of a voltage-dependent process, premature slow waves may result from the activation of a voltage-dependent ionic conductance. Activation of voltage-dependent ion channels with short duration pulses is common, depending upon the time constants of cells in which the ion channels are expressed. Pacemaker ICC express dihydropyrdine-insensitive Ca^{2+} channels (low-voltage-activated) that might be activated by impulses of brief depolarization (Lee & Sanders, 1993; Kim *et al.* 2002). We suggest that Ca^{2+} entry via such a mechanism might increase the open probability of IP_3 receptors and phase advance slow waves. It should be noted that an intermediate explanation is also possible in which Ca^{2+} entry (which might be activated by brief pulses of EFS but result in a relatively more sustained rise in Ca^{2+} due to slower extrusion and/or uptake mechanisms) might activate Ca^{2+}-dependent phospholipase enzymes and phase advance slow waves by production of IP_3. The significant time delays between depolarization and generation of regenerative potentials in ICC-IM/smooth muscle bundles seems to favour a multi-step process coupling depolarization to initiation of pacemaker currents (Hirst *et al.* 2002*b*).

The phasic contractile activity of GI muscles has been proposed to be the result of the integrated responses of at least four types of cells: (i) enteric motor neurons, (ii) ICC-IM/ICC-SEP, smooth muscle cells and ICC-MY (Horowitz *et al.* 1999). Slow waves, generated in primary pacemaker networks such as ICC-MY, are actively propagated through ICC networks that spread around and along GI organs. Electrical coupling between pacemaker ICC and circular and longitudinal muscle cells facilitates conduction (i.e. passive spread) of depolarizing currents from the ICC network to smooth muscle cells. Depolarization of smooth muscle cells activates L-type Ca^{2+} channels, which results in sufficient Ca^{2+} entry to activate the contractile apparatus. This is the main excitation–contraction coupling step coupling slow waves to phasic (peristaltic) contractions. The magnitude of coupling between slow waves and L-type channels depends upon the level and duration of depolarization achieved during slow waves, and the voltage responses of the smooth muscle syncytium is regulated by local neural, hormonal and paracrine stimulation. Neural responses were largely missing in W/W^V muscles, demonstrating the importance of ICC-IM in mediating neural regulation of slow wave activity.

Our pacing experiments predict certain restrictions on the use of gastric pacing to elicit or organize slow waves in patients with damaged ICC networks, a condition occurring in a variety of motility disorders (Vanderwinden *et al.* 1996*a*,*b*; Sanders *et al.* 1999). We have suggested that loss of ICC may contribute to gastropathies that are often associated with diabetes (Ordog *et al.* 2000). Associated with reduced neural responses in the stomachs of non-obese diabetic (NOD) mice there is a profound reduction in the number of ICC-IM in the circular muscle layer of the gastric antrum and a significant disruption in the normally close association between enteric nerve terminals and ICC-IM. Hence, it is unlikely that short stimulation pulses with durations in the order of 0.1 ms would be sufficient to regulate slow wave frequency in patients with certain gastropathies.

REFERENCES

Banks BE, Brown C, Burgess GM, Burnstock G, Claret M, Cocks TM & Jenkinson DH (1979). Apamin blocks certain neurotransmitter-induced increases in potassium permeability. *Nature* **282**, 415–417.

Beckett EA, Horiguchi K, Khoyi M, Sanders KM & Ward SM (2002). Loss of enteric motor neurotransmission in the gastric fundus of Sl/Sl(d) mice. *J Physiol* **543**, 871–887.

Journal of Physiology

Bortolotti M (2002). The 'electrical way' to cure gastroparesis. *Am J Gastroenterol* **97**, 1874–1883.

Burns AJ, Lomax AE, Torihashi S, Sanders KM & Ward SM (1996). Interstitial cells of Cajal mediate inhibitory neurotransmission in the stomach. *Proc Natl Acad Sci U S A* **93**, 12008–12013.

Daniel EE, Posey-Daniel V (1984). Neuromuscular structures in opossum esophagus: role of interstitial cells of Cajal. *Am J Physiol* **246**, G305–315.

Dickens EJ, Edwards FR & Hirst GD (2001). Selective knockout of intramuscular interstitial cells reveals their role in the generation of slow waves in mouse stomach. *J Physiol* **531**, 827–833.

Dickens EJ, Hirst GD & Tomita T (1999). Identification of rhythmically active cells in guinea-pig stomach. *J Physiol* **514**, 515–531.

Edwards FR, Hirst GD & Suzuki H (1999). Unitary nature of regenerative potentials recorded from circular smooth muscle of guinea-pig antrum. *J Physiol* **519**, 235–250.

Epperson A, Hatton WJ, Callaghan B, Doherty P, Walker RL, Sanders KM, Ward SM & Horowitz B (2000). Molecular markers expressed in cultured and freshly isolated interstitial cells of Cajal. *Am J Physiol Cell Physiol* **279**, C529–539.

Hirst GD, Beckett EA, Sanders KM & Ward SM (2002*a*). Regional variation in contribution of myenteric and intramuscular interstitial cells of Cajal to generation of slow waves in mouse gastric antrum. *J Physiol* **540**, 1003–1012.

Hirst GD, Bramich NJ, Teramoto N, Suzuki H & Edwards FR (2002*b*). Regenerative component of slow waves in the guinea-pig gastric antrum involves a delayed increase in $[Ca^{2+}]_i$ and Cl^- channels. *J Physiol* **540**, 907–919.

Hirst GD, Dickens EJ & Edwards FR (2002*c*). Pacemaker shift in the gastric antrum of guinea-pigs produced by excitatory vagal stimulation involves intramuscular interstitial cells. *J Physiol* **541**, 917–928.

Horiguchi K, Semple GS, Sanders KM & Ward SM (2001). Distribution of pacemaker function through the tunica muscularis of the canine gastric antrum. *J Physiol* **537**, 237–250.

Horowitz B, Ward SM & Sanders KM (1999). Cellular and molecular basis for electrical rhythmicity in gastrointestinal muscles. *Annu Rev Physiol* **61**, 19–43.

Kelly KA & La Force RC (1972). Pacing the canine stomach with electric stimulation. *Am J Physiol* **222**, 588–594.

Kim TW, Beckett EA, Hanna R, Koh SD, Ordog T, Ward SM & Sanders KM (2002). Regulation of pacemaker frequency in the murine gastric antrum. *J Physiol* **538**, 145–157.

Koh SD, Dick GM & Sanders KM (1997). Small-conductance Ca(2+)-dependent K^+ channels activated by ATP in murine colonic smooth muscle. *Am J Physiol* **273**, C2010–2021.

Ladabaum U & Hasler WL (1999). Novel approaches to the treatment of nausea and vomiting. *Dig Dis* **17**, 125–132.

Lee HK & Sanders KM (1993). Comparison of ionic currents from interstitial cells and smooth muscle cells of canine colon. *J Physiol* **460**, 135–152.

Lin ZY, McCallum RW, Schirmer BD & Chen JD (1998). Effects of pacing parameters on entrainment of gastric slow waves in patients with gastroparesis. *Am J Physiol* **274**, G186–191.

McCallum RW (1987). Gastric emptying disorders. Tests and treatments. *Postgrad Med* **81**, 67–76.

McCallum RW, Chen JD, Lin Z, Schirmer BD, Williams RD & Ross RA (1998). Gastric pacing improves emptying and symptoms in patients with gastroparesis. *Gastroenterology* **114**, 456–461.

Mahaut-Smith MP, Hussain JF & Mason MJ (1999). Depolarization-evoked Ca^{2+} release in a non-excitable cell, the rat megakaryocyte. *J Physiol* **515**, 385–390.

Miedema BW, Sarr MG & Kelly KA (1992). Pacing the human stomach. *Surgery* **111**, 143–150.

Nose K, Suzuki H & Kannan H (2000). Voltage dependency of the frequency of slow waves in antrum smooth muscle of the guinea-pig stomach. *Jpn J Physiol* **50**, 625–633.

Ordog T, Baldo M, Danko R & Sanders KM (2002). Plasticity of electrical pacemaking by interstitial cells of Cajal and gastric dysrhythmias in W/W mutant mice. *Gastroenterology* **123**, 2028–2040.

Ordog T, Takayama I, Cheung WK, Ward SM & Sanders KM (2000). Remodeling of networks of interstitial cells of Cajal in a murine model of diabetic gastroparesis. *Diabetes* **49**, 1731–1739.

Ordog T, Ward SM & Sanders KM (1999). Interstitial cells of cajal generate electrical slow waves in the murine stomach. *J Physiol* **518**, 257–269.

Ozaki H, Stevens RJ, Blondfield DP, Publicover NG & Sanders KM (1991). Simultaneous measurement of membrane potential, cytosolic Ca^{2+}, and tension in intact smooth muscles. *Am J Physiol* **260**, C917–925.

Roman C, Gonella J, Niel JP, Condamin M & Miolan JP (1975). Effets de la stimulation vagale et de l'adrenaline sur la musculeuse lisse du bas oesophage du chat. *INSERM* **50**, 415–422.

Rumessen JJ, Mikkelsen HB, Qvortrup K & Thuneberg L (1993). Ultrastructure of interstitial cells of Cajal in circular muscle of human small intestine. *Gastroenterology* **104**, 343–350.

Sanders KM, Ordog T, Koh SD, Torihashi S & Ward SM (1999). Development and plasticity of interstitial cells of Cajal. *Neurogastroenterol Motil* **11**, 311–338.

Sarna SK & Daniel EE (1973). Electrical stimulation of gastric electrical control activity. *Am J Physiol* **225**, 125–131.

Suzuki H & Hirst GD (1999). Regenerative potentials evoked in circular smooth muscle of the antral region of guinea-pig stomach. *J Physiol* **517**, 563–573.

Suzuki H, Ward SM, Bayguinov YR, Edwards FR & Hirst GD (2003). Involvement of intramuscular interstitial cells in nitrergic inhibition in the mouse gastric antrum. *J Physiol* **546**, 751–763.

Tomita T (1981). Electrical activity (spikes and slow waves) in gastrointestinal smooth muscle. In *Smooth Muscle: An Assessment of Current Knowledge*, ed. Bulbring E, Brading AF, Jones AW & Tomita T, pp. 127–156. University of Texas Press, Austin, Texas, USA.

Torihashi S, Kobayashi S, Gerthoffer WT & Sanders KM (1993). Interstitial cells in deep muscular plexus of canine small intestine may be specialized smooth muscle cells. *Am J Physiol* **265**, G638–645.

Vanderwinden JM, Liu H, De Laet MH & Vanderhaeghen JJ (1996*a*). Study of the interstitial cells of Cajal in infantile hypertrophic pyloric stenosis. *Gastroenterology* **111**, 279–288.

Vanderwinden JM, Rumessen JJ, Liu H, Descamps D, De Laet MH & Vanderhaeghen JJ (1996*b*). Interstitial cells of Cajal in human colon and in Hirschsprung's disease. *Gastroenterology* **111**, 901–910.

Van Helden DF, Imtiaz MS, Nurgaliyeva K, von der Weid PY & Dosen PJ (2000). Role of calcium stores and membrane voltage in the generation of slow wave action potentials in guinea-pig gastric pylorus. *J Physiol* **524**, 245–265.

Vogalis F & Goyal RK (1997). Activation of small conductance Ca(2+)-dependent K^+ channels by purinergic agonists in smooth muscle cells of the mouse ileum. *J Physiol* **502**, 497–508.

Wang XY, Sanders KM & Ward SM (1999). Intimate relationship between interstitial cells of Cajal and enteric nerves in the guinea-pig small intestine. *Cell Tissue Res* **295**, 247–256.

Ward SM, Beckett EA, Wang X, Baker F, Khoyi M & Sanders KM (2000*a*). Interstitial cells of Cajal mediate cholinergic neurotransmission from enteric motor neurons. *J Neurosci* **20**, 1393–1403.

Ward SM, Ordog T, Koh SD, Baker SA, Jun JY, Amberg G, Monaghan K & Sanders KM (2000*b*). Pacemaking in interstitial cells of Cajal depends upon calcium handling by endoplasmic reticulum and mitochondria. *J Physiol* **525**, 355–361.

Ward SM & Sanders KM (2001). Interstitial cells of Cajal: primary targets of enteric motor innervation. *Anat Rec* **262**, 125–135.

Acknowledgements

The authors are grateful for the technical assistance of Julia Bayguinov for immunohistochemical studies, Emma Wade for assistance with electrophysiological studies and Andrea Liggett for analysis. Experiments were supported by DK 57236. Morphological studies were supported by the Core laboratory facility of a Program Project Grant (DK 41315).

Journal of Physiology